Oxford INCA Energy Dispersive Spectrometer (EDS)

Training Guide

The text of this training guide was taken primarily from Scanning Electron Microscopy and X-ray Microanalysis, 3rd Ed. Goldstein, J.; Newbury, D.; Joy, D.; Lyman, C.; Echlin, P. Lifshin, E.; Sawyer, L.; Michael, J. 2003, Springer, New York, NY.

How are X-rays generated?

In the SEM, beam electrons of sufficient energy can interact with the tightly bound inner shell electrons of a specimen atom, ejecting an electron from a shell. The atom is left as an ion in an excited, energetic state, as shown in Figure 1. The incident beam electron leaves the atom having lost at least E_K, where E_K is the binding energy of the electron to the *K* shell. The ejected orbital electron leaves the atom with a kinetic energy of a few eV to several keV, depending on the interaction. The atom itself is left in the excited state with a missing inner shell electron. The atom relaxes to its ground state (lowest energy) within approximately 1 ps through a limited set of allowed transitions of outer shell electron(s) filling the inner-shell vacancy. The energies of electrons in the shells (atomic energy levels) are sharply defined with values characteristic of a specific element. The energy difference between electron shells is a specific or characteristic value for each element. The excess energy can be released from the atom during relaxation in one of two ways (two branches of Figure 1). In the Auger process, the difference in shell energies can be transmitted to another outer shell electron, ejecting it from the atom as an electron with a specific kinetic energy. In the characteristic x-ray process, the difference in energy is expressed as a photon of electromagnetic radiation which has a sharply defined energy. For the case of the neon atom shown schematically in Figure 1, creation of a *K*-series x-ray involves filling the vacant state in the innermost electron shell (*K* shell) with an electron transition from the next shell out (*L* shell). Thus, the energy of the K_α x-ray produced is equal to the difference in energy between the K shell and the L shell.

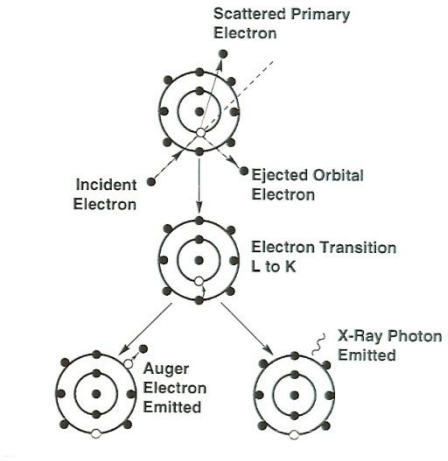

Figure 1. Inner shell electron ionization in an atom and subsequent de-excitation by electron transitions. The incident electron is elastically scattered. The difference in energy from an electron transition is expressed either as the ejection of an energetic electron with characteristic energy (Auger process) or by the emission

Beam electrons can also undergo deceleration in the Coulombic field of the specimen atoms, which is the positive field of the nucleus modified by the negative field of the bound electrons. The loss in electron energy ΔE that occurs in such a deceleration event is emitted as a

photon. This radiation is referred to as bremsstrahlung, or "braking radiation". Because the interactions are random, the electron may lose any amount of energy in a single deceleration event. Therefore, the bremsstrahlung can take on any energy value from zero up to the original energy of the incident electron E_0, forming a continuous electromagnetic spectrum. Figure 2 shows the x-ray spectrum of copper including the characteristic peaks from copper and the continuum bremsstrahlung x-rays.

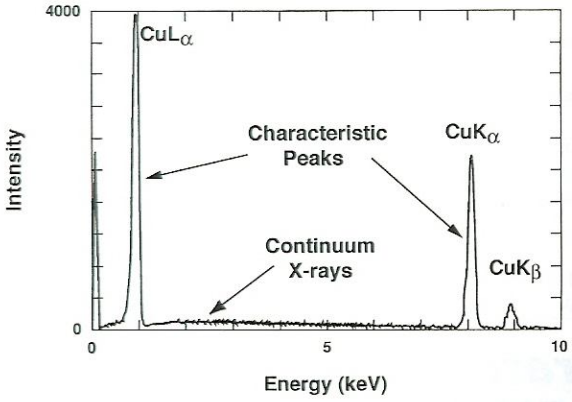

Figure 2. X-ray spectrum of copper showing *K*-series and *L*-series x-ray peaks and the continuous x-ray spectrum (bremsstrahlung or continuum) obtained with a Si(Li) EDS detector with an ultrathin (diamond) x-ray window. Natural widths of peaks are much narrower than measured here. A noise peak is measured at very low energies.

X-ray Transitions Nomenclature

Electrons of an atom occupy electron shells around the atom that have specific energies. In order of increasing distance from the atomic nucleus, these shells are designated the *K* shell, the *L* shell, the *M* shell, etc. These shells are directly related to the quantum numbers of atomic physics. For shells beyond the *K* shell, the shells are divided into subshells. For example, the *L* shell is composed of three subshells that are closely spaced in energy, and the *M* shell has five subshells. Figure 3 shows a simplified energy-level diagram that illustrates the nomenclature for x-ray emission lines. For elements with atomic numbers ≥ 11 (sodium), the shell structure is sufficiently complex that when an ionization occurs in the *K* shell, the transition to fill that vacant state can occur from more than one outer shell. As shown in Figure 3, following ionization of a *K* shell electron, a transition to fill the vacant state can occur from either the *L* shell or the *M* shell. X-rays resulting from transitions of electrons from the *M* shell to the *K* shell are designated K_β x-rays. Because the energy difference between the *K* and *M* shells is larger than between the *K* and *L* shells, the K_β x-ray energy is larger than that of the K_α. For example, for copper, the K_α x-ray has an energy of 8.04 keV and the K_β x-ray has an

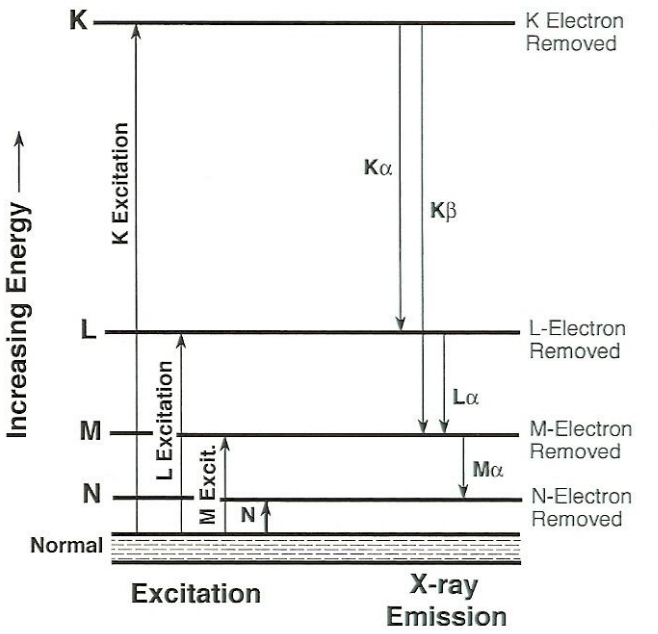

Figure 3. Energy level diagram for an atom. The energy of the atom increases upon ionization of the *K*, *L*, *M*, or *N* shell (excitation). As the atom's energy returns to normal, K_α, K_β, L_α, and M_α x-rays are emitted from the atom. Each horizontal line represents the energy of an electron state. Zero energy represents an atom at rest with no electrons missing (normal).

energy of 8.90 keV. (For more x-ray lines, see Appendix B.)

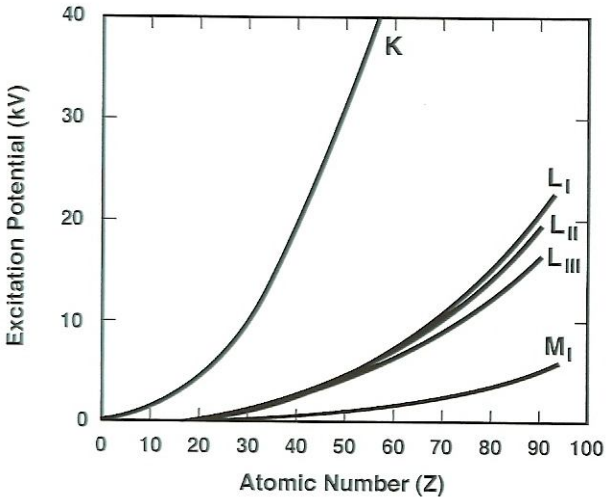

Figure 4. Critical excitation energies (absorption edge energies) for the *K*, *L*, and *M* series as a function of atomic number.

Because the energy of each shell and subshell is sharply defined, the minimum energy necessary to remove an electron from a specific shell has a sharply defined value as well. This energy is called the critical ionization or excitation energy E_c, also known as the excitation potential or x-ray absorption edge energy. Figure 4 shows the critical excitation energies for the *K*, *L*, and *M* series as a function of atomic number (For a table of E_c values, see Appendix A). As an example, consider the wide range in critical ionization energies for the *K*, *L*, and *M* shells and subshells of platinum (Z = 78). A 20 keV electron beam can ionize the *L* and *M* shells of Pt, but not the *K* shell. As the atomic number decreases, the ionization energies decrease. Primary ionization involves removing an electron from a bound state in a shell to an effective infinity outside the atom. However, characteristic x-rays are formed by transitions between bound states in shells. Therefore, the energy of the characteristic x-ray is always less than the critical ionization energy for the shell from which the original electron was removed (see Figure 3).

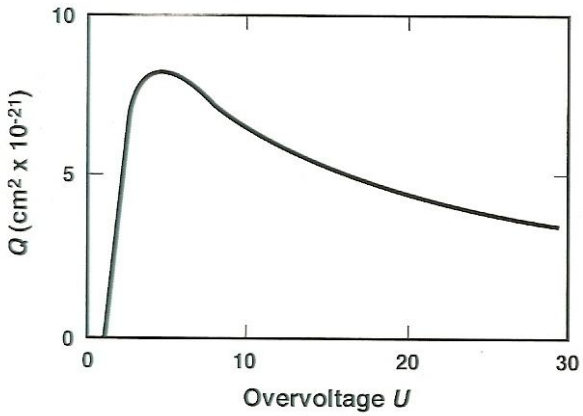

Figure 5. Plot of the cross section for inner shell ionization of the silicon *K* shell as a function of overvoltage $U = E/E_c$.

Ideally the accelerating voltage (V_{acc}) is set at 2-3 times the critical ionization energy of the elements of interest. The overvoltage (U) is defined as the ratio between the beam energy (E or V_{acc}) and the critical excitation energy ($U = E / E_c$). The cross section, or the probability for inner shell ionization, depends on the overvoltage as shown in Figure 5. The cross section increases with overvoltage and then peaks at around U = 3 before declining. Thus, working within this ideal overvoltage range is preferred.

Fluorescence yield

The partitioning of the de-excitation process between the x-ray and Auger branches (Figure 1) is described by the fluorescence yield, ω.

$$\omega_K = \frac{\#\,K\ photons\ produced}{\#\,K\text{-}shell\ ionizations} \qquad (1)$$

The x-ray process is not favored for low atomic numbers; for example, $\omega_K \sim 0.005$ for the carbon *K* shell (Figure 6). The characteristic x-ray process dominates for high atomic numbers; for example, $\omega_K \sim 0.5$ for germanium, increasing to near unity for the heaviest elements. The fluorescence yields of the *L* and *M* shells are also shown in Figure 6.

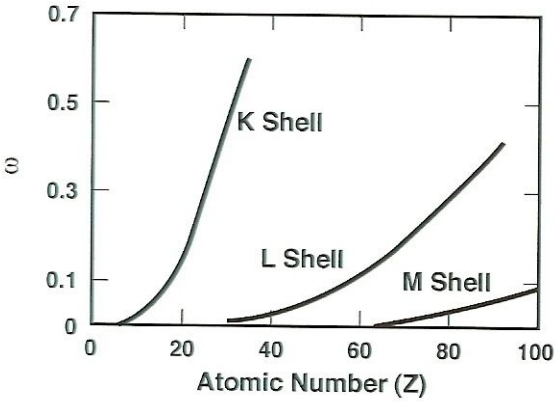

Figure 6. Fluorescence yield ω as a function of atomic number for electron ionization within the *K*, *L*, and *M* electron shells.

Spatial & Depth Resolution

Depending on the critical excitation energy E_c, characteristic x-rays may be generated over a substantial fraction of the electron interaction volume. To predict the depth of x-ray production (x-ray range) and the lateral x-ray source size (x-ray spatial resolution), the starting point is the electron range. *Electron* range (*R*) expressions have the following general form:

$$\rho R = K(E_0^n - E_c^n) \tag{2}$$

Where E_0 is the incident electron beam energy, ρ is the density, *K* depends on material parameters, and *n* is a constant between 1.2 and 1.7.

Characteristic x-rays can only be produced within that portion of the electron trajectories for which the energy exceeds E_c for a particular x-ray line. The range of direct primary x-ray generation is therefore always smaller than the electron range. The higher E_0, and the less dense the sample, the further electrons will penetrate into the sample. By fitting Equation 2 to experimental data, Anderson and Hasler[1] evaluated the constants *K* and *n*, obtaining an analytical expression for the *x-ray* range useful for most elements:

$$R_x = \frac{0.064}{\rho}(E_0^{1.68} - E_c^{1.68}) \tag{3}$$

where R_x has units of μm, when *E* is in keV and ρ is in g/cm^3.

For an electron beam normal to a surface, the maximum width of the electron interaction volume or x-ray generation volume projected up to the specimen surface is approximately equal to the spatial resolution. Figure 7 shows how the x-ray range and the x-ray spatial resolution L_x are defined in cross section. As the atomic number and density of the target increase, the depth of production for the principal line decreases. The depth of production is also a function of the critical ionization energy of the line. These effects are shown in Figure 7. For the same beam energy the figure shows how the x-ray range and the x-ray spatial resolution vary for Al K_α and Cu K_α in a matrix of density ~3g/cm^3 (e.g., aluminum) and in a matrix of density ~10 g/cm^3

(e.g., copper). In the low-density sample, a trace amount of Cu is present in an Al sample, whereas in the high-density sample, a trace element amount of Al is present in a Cu sample. Both Al K_α and Cu K_α are produced at greater depths in the low density matrix than in the high-density matrix. The shapes of the interaction and x-ray generation volumes differ considerably in the two targets, with the low-density matrix having a pear shape and the high-density matrix giving a less distinct neck.

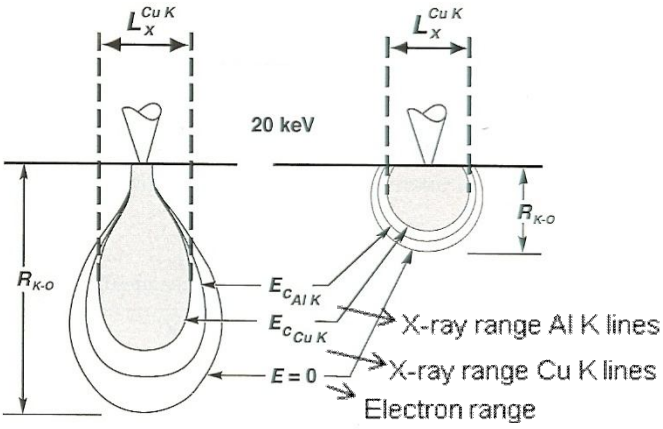

Figure 7. Comparison of x-ray production regions from specimens with densities of 3 g/cm^3 (left) and 10 g/cm^3 (right) at a beam energy of 20 keV. The x-ray spatial resolution L_x is found by projecting the maximum diameter of the x-ray distribution to the surface of the specimen.

X-ray Absorption

X-rays, as photons of the electromagnetic radiation, can undergo the phenomenon of photoelectric absorption upon interacting with an atom. That is, the photon is absorbed and the energy is completely transferred to an orbital electron, which is ejected with a kinetic energy equal to the photon energy minus the binding energy (critical ionization energy) by which the electron is held to the atom. Fortunately, there is no change in the energy of the x-ray photon that passes through the absorber. Typical values of mass absorption coefficients (μ/ρ) for Cu K_α radiation traveling through various pure elements are listed in Table 1. Note that for Cu K_α radiation the mass absorption coefficient is high for Co as an absorber. The energy of Cu K_α is slightly higher than E_c for Co, but is much lower than E_c for Cu as an absorber. Because the energy of an element's characteristic radiation is always less than E_c, the absorption coefficient of an element for its own radiation is low. Therefore, an element passes its own characteristic line with little absorption.

Table 1. Mass Absorption Coefficient (μ/ρ) of Several Elements for Cu K_α

Element (atomic number)	X-ray energy (keV)			(μ/ρ) of Cu $K\alpha$ in given element (cm^2/g)
	$K\alpha$	$K\beta$	$E_c = E_{K\,edge}$	
Mn (25)	5.895	6.492	6.537	272
Fe (26)	6.400	7.059	7.111	306
Co (27)	6.925	7.649	7.709	329
Ni (28)	7.472	8.265	8.331	49
Cu (29)	8.041	8.907	8.980	52

Photoelectron absorption by electrons in a specific shell requires that the photon energy exceed the electron binding energy for that shell. When the photon energy is slightly greater than the binding energy of the electron in the absorber (E_c), the probability for absorption is highest. For a specific absorber, mass absorption coefficients generally decrease in a smooth fashion with increasing x-ray energy. However, there is a sharp jump in absorption coefficient in the energy region just greater than the critical excitation energy for each shell of the absorber.

Figure 8 shows a plot of the mass absorption coefficeient (μ/ρ) for the element lanthanum (Z=57) as an absorber of various x-ray energies. Sharp jumps in (μ/ρ) occur at the energy of the *K* edge at 38.9 keV, the *L* edges at ~5.9 keV, and the M edges at ~1.1 keV. These jumps are referred to as "x-ray absorption edges". X-rays with an energy slightly greater than the x-ray absorption edge (critical ionization energy) can eject a bound electron and therefore are strongly absorbed themselves.

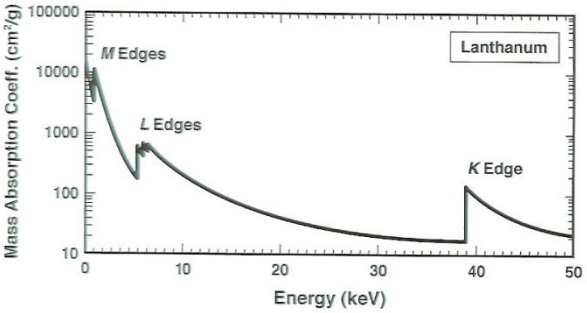

Figure 8. Mass absorption coefficient as a function of x-ray energy in an absorber of lanthanum (atomic number 57).

Absorption edges can be directly observed when the x-ray spectrum energy range spans the critical excitation energy for the absorber element in the target. The electron-excited x-ray bremsstrahlung provides a continuous distribution in energy. At the absorption edge, the bremsstrahlung intensity abruptly decreases for x-ray energies slightly above the edge because the mass absorption coefficient increases abruptly at the absorption edge. An example for nickel excited with a 40 keV electron beam is shown in Figure 9. Just above the Ni K_α and Ni K_β lines, at the position of the critical excitation energy for the Ni *K* shell ($E_c = E_K = 8.33$ keV), the x-ray bremsstrahlung is much lower than what would be expected if the bremsstrahlung below the peaks were extrapolated to higher energy. This sudden decrease in the continuum corresponds to a sudden increase in the mass absorption coefficient for Ni. The presence of absorption edges in spectra may be difficult to observe if they are hidden under an x-ray peak that has been broadened by the detection process as is often the case in EDS analysis.

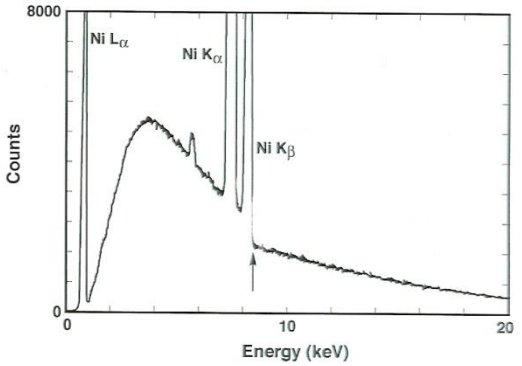

Figure 9. Energy-dispersive x-ray spectrum of nickel generated with a primary electron beam energy of 40 keV. The spectrum shows a sharp step in the x-ray continuum background due to increased absorption just above the Ni *K* absorption edge (arrow).

X-ray Fluorescence

For some element pairs in the specimen the primary x-ray of element A created by the electron beam can generate a secondary x-ray of element B by fluorescence. This process is an inevitable consequence of photoelectric absorption of primary A x-rays by a specimen B atom with the ejection of a bound inner shell electron from the absorbing B atom. The primary A photon is absorbed by the specimen B atom and its energy is transferred to the kinetic energy of the ejected electron, the photoelectron. The B atom is left in the same excited state as that produced by inner shell ionization directly by the electron beam. Subsequent deexcitation as the atom returns to the ground state by electron transitions is the same for both cases: The excited

atom will follow the same routes to deexcitation, producing either characteristic x-rays or characteristic electrons (Auger electrons). X-ray induced emission of x-rays is referred to as "x-ray fluorescence".

The Detection Process

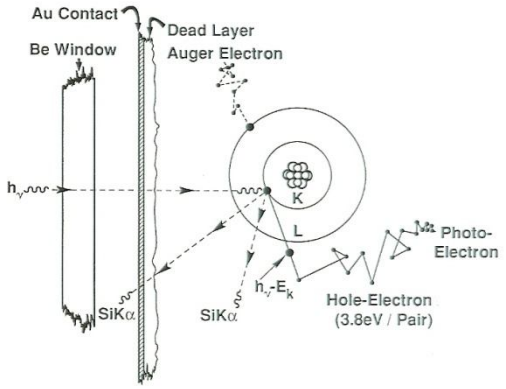

Figure 10. The x-ray detection process in the Si(Li) detector.

The basic detection process by which the photon energy is converted into an electrical signal is illustrated in Figure 10. The active portion of the detector consists of intrinsic silicon with a thin layer of p-type material on the front surface, called the "dead layer", coated with a thin gold electrical contact. When an energetic photon is captured, electrons are promoted into the conduction band, leaving holes in the valence band. Under an applied bias, these electrons and holes are swept apart and collected on the electrodes on the faces of the crystal. The process of x-ray capture is photoelectric absorption, and the x-ray photon is annihilated in the process. The incident x-ray photon with an energy hν is first absorbed by a silicon atom and an inner shell electron is ejected with an energy $h\nu - E_c$, where E_c for silicon is 1.84 keV. This photoelectron then creates electron-hole pairs as it travels in the detector silicon and scatters inelastically. The silicon atom is left in an excited state because of the vacancy caused by the ejection of the photoelectron. As electrons from less tightly bound states fill the vacancy, energy is subsequently released in the form of either an Auger electron or a silicon x-ray. The Auger electron scatters inelastically and also creates electron-hole pairs. The silicon x-ray can be reabsorbed, which initiates the process again, or it can be scattered inelastically. Thus, a sequence of events takes place leading to the deposition of all of the energy of the original photon in the detector, unless radiation generated during the sequence, such as a silicon K_α photon, escapes the detector giving rise to the artifact known as the "escape peak".

The ideal number of charges *n* created in the detector per incident photon with energy E (eV) is given by

$$n = E/\varepsilon \tag{4}$$

Where ε = 3.86eV for Si at 77K. For example, if the detector captures one photon having an energy of 5 keV, then from the above equation, the total number of electrons swept from the detector is approximately 1300, which represents a charge of 2×10^{-16} C. This is an extraordinarily small charge. To measure charge accurately, noise minimization is essential, hence the need for keeping the detector crystal close to liquid nitrogen temperature to reduce thermal noise contributions.

Once created, the charge from the detector goes through a charge-to-voltage converter. The output voltage for each incident x-ray is a voltage which is proportional to the incident photon energy. The signal then goes through a pulse shaping amplifier which converts the voltage steps into peaks. To accurately measure the voltage step, the noise on either side of the voltage step needs to be averaged. Up to a point, increasing the time (process time on our EDS software) that the noise level is analyzed improves the accuracy of the pulse height as a measure of the energy of the originating x-ray photon. In order to accomplish this, however, voltage step times have to be extended to several or even tens of microseconds. This can cause a problem, called "pulse pileup", if the number of photons entering the detector exceeds a few thousand per second. Pulse pileup occurs if a photon arrives at the detector before the linear amplifier is finished processing the preceding photon. It appears as an increased output pulse height for the second photon because it is riding on the tail of the first. In the most extreme case, two photons arrive at the detector almost simultaneously, and the output is a single combined pulse corresponding to the sum of the two photon energies. This phenomenon gives rise to what are called "sum peaks" (or "coincidence peaks") such as the $2K_\alpha$ and the $K_\alpha + K_\beta$ peaks. Table 2 qualitatively describes the differences that process time can have on various spectral parameters.

Table 2. Effect of Process Time on Spectral Parameters

Characteristic	**Low Process time** ⟷ **High Process time**
Peak FWHM (spectral resolution)	Wide Peaks ⟷ Narrow Peaks
Pulse pileup	Few Sum Peaks ⟷ More Sum Peaks
Deadtime %	Low Deadtime % ⟷ High Deadtime %

Quantitative Analysis

Coming soon…

[1] Anderson, C.A.; Hasler, M.F. *Proceedings of the 4th International Conference on X-ray Optics and Microanalysis* (Castaing, R.; Deschamps, P.; Philibert, J. eds.). Hermann, Paris, p.310.